Thermal Effect of the Slanted Surface around the Central Hole of a Miniature Delta Wing on the Leading-edge Vortices

Chin-Tsan Wang [1,*] and Tzong-Shyng Leu[2]

[1]Department of Mechanical and Electro-Mechanical Engineering

National I Lan University / 1, Sec. 1, Shen-Lung Road, I-Lan, 26047, Taiwan

[2]Department of Aeronautics and Astronautics

National Cheng Kung University / 1, Ta-Hsueh Road, Tainan 70101, Taiwan

* Author to whom correspondence should be addressed; E-Mail: ctwang@niu.edu.tw; Tel.: +886-3-9357400, ext 686; Fax: +886-3-9311326

Abstract: The main feature of a delta wing is in the generation of vortices on the leading edge of its wings to provide additional stable lift at high angle of attack. The main purpose of this study is to analyze the impact of lee side central holes under thermal condition to the development of vortex flow field at the tip of a miniature delta wing and find the region with the most significant changes in the velocity and pressure gradient to serve as the thermal control location of a future delta wing. The study chooses near wing surface heat flux of $Q=100W/m^2$ and $10W/m^2$, representing the high and the low heat flux, at Reynolds number, $Re=2.64\times10^3$ and 8.84×10^3, to perform flow field analysis. The study finds: the temperature effect under the high heat flux produces a significant impact on the angle of attack (AOA) and the angle of sideslip (AOS) of the delta wing and can easily cause the occurrence of asymmetric flow field of vortices at the downstream tip of the delta wing. Additionally, because a significant velocity and pressure gradient exist around the corner on the bottom slanted surface of the lee side central hole in the delta wing, the temperature impact on the change of AOA is most pronounced and it is also the region of which the development of vortex flow field is most affected. These findings could provide information on realizing the thermal effect on the leading-edge vortices over the miniature delta wing for future optimal flow control.

Key-Words: delta wing, angle of attack, angle of sideslip, thermal control, heat flux, vortex flow, thermal effect

1 Introduction

Control of vortices over slender delta wings at high angles of attack is dependent on the knowledge and on the ability to detect or observe the principle characteristics of the phenomenon. Substantial theoretical, experimental and numerical researches have focused on the characteristics of leading edge vortices and vortex breakdown. The vortex flow characteristics of a sharp-edged delta wing at high angles of attack were studied using a computational technique. Three dimensional, compressible Reynolds-averaged Navier-Stokes equations were solved to understand the effects of the angle of yaw, angle of attack, and free stream velocity on the development and interaction of vortices and the relationship between suction pressure distributions and vortex flow characteristics [1]. On the vortex dynamics of free-to-roll slender and nonslender delta wings, experiments were conducted on various free-to-roll delta wings with sweep angles in the range of 40-70 deg in a wind tunnel. The magnitude of the roll trim angle decreases with increasing sweep angle and almost disappears for the most slender wing [2]. Surface streamlines and normal-to-plane motion adjacent to a delta-wing platform has been reported [3]. Elkhoury and Nakad indicated that control at the trailing edge has a global effect on buffet loading and three-dimensional flow separation [3]. The leading-edge vortex of delta wing can not only improve the wing's aerodynamic characteristics, but also affect its aeroelastic characteristics. The results show that the leading-edge vortex has a significant impact on the flutter characteristics of that delta wing [4]. However, there are quite a few studies related to the cold and thermal flow field simulations and experiments of delta wing: such as the study of the impact of heat transfer by the longitudinal vortices

generated by the semi-delta wing in Eibeck and Eaton [5], and the study of the heat flux of a pair of semi-delta wings in Pauley and Eaton [6] etc. The results show: when the secondary current flows towards the wall surface, the heat transfer effect will be enhanced; while it flows away from the wall surface, the thermal effect will be reduced. Fiebig [7] points out: there is strong longitudinal vortex current behind the vortex generator of a delta wing. When this secondary current flows towards the wall surface, the heat transfer of the wall surface will be enhanced to achieve the objective of reducing the wall temperature. As a result, the efficiency of heat transfer of the whole pipeline can be boosted. In addition, aerodynamic heating will result in changes in the natural dynamic characteristics of the models, so the flutter velocity of the delta wing will decline sharply [8]. According to the boundary layer theory, the separation state of the boundary layers at the leading edge of a delta wing will change under the disturbance of a micro-actuator. The leading edge vortices on both sides of the lee side of a delta wing will be distributed symmetrically without the disturbance of the actuator. On the other hand, if the micro-actuator agitates before the original separation point (assuming the micro-actuator is placed on the left front edge) causing the early separation of the boundary layers, the vortex core will move towards the outer flank of the wings. The corresponding vortex lifting torque on the flank will increase accordingly and produce a clockwise rolling torque. If the micro-actuator agitates behind the original separation point causing the late separation of the boundary layers, the vortex core will move inward causing the reduction of the vortex lifting torque on the same side. And the wing will obtain a counter clockwise rolling torque. Micro-actuator array not only can achieve rolling control, but also can produce torque to control the manoeuvring actions of a delta wing such as pitching, and yawing, etc. through the judicious placement of the micro-actuator array. Therefore, this study will analyze the impact of the thermal effect of the central hole to the wing tip vortices in a miniature delta wing and find the region with the most pronounced change of the velocity and pressure gradient as the thermal control point for a future optimal design of delta wing.

2 Simulation Analysis

This study investigates the impact of the thermal effect of the slanted surfaces around the central hole of a miniature delta wing on the leading-edge vortices development by using numerical simulation methods to identify the region with the most pronounced changes of the flow field for future flow control.

The physical model is a miniature delta wing with a height of 123.49mm and a base of 200mm; the square slanted central hole has a length of 25mm on each side and a 26 degrees slanted surface towards the bottom. The geometric shape of the delta wing is shown in Fig.1.

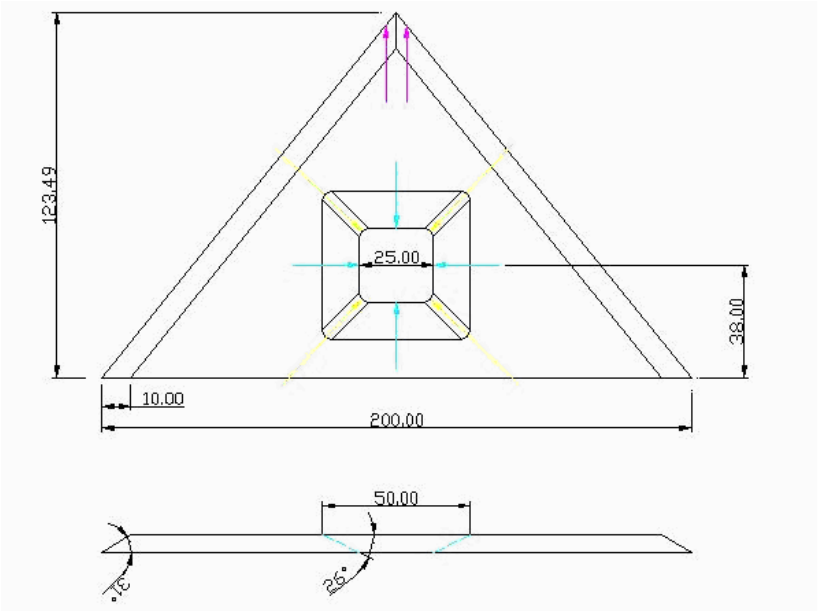

Fig.1 The diagram of the geometry of miniature delta wing (unit: mm)

The computation domain whose dimension is 90cm×90cm×24cm respectively was applied for the delta wing and currents with uniform flow velocity of V_{inlet}= 0.34m/s and 1.1378m/s are introduced respectively at the entrance as inputs. The flow field boundary conditions are set to relative Reynolds numbers of Re = 2.64×10^3 and 8.84×10^3 and the rest of the boundary conditions are set to fixed pressure with 1 atmospheric pressure, as shown in Fig.2.

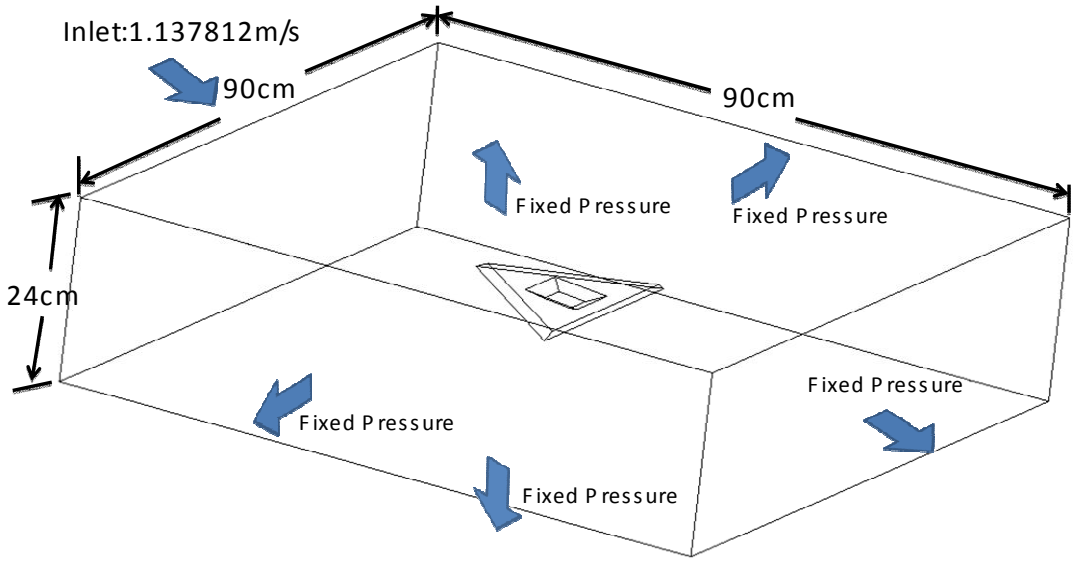

Fig.2 The computation domain and the boundary conditions applied to simulation

In this study, the simulation was performed with the CFD-ACE+ software (CFD Research Corporation, Huntsville Alabama), a multi-physics package based on the Finite-Volume methods [9, 10]. The program would be run on a 2.4 GHz Pentium IV processor with 1GB of RAM memory. The mesh-independent test runs were made before the study. To perform numerical analysis, CFDRC numerical simulation software would be adopted to conduct the flow field analysis. Local mesh refinement is applied to areas with large geometric variations on the delta wing using first-order upwind solver method with structural and non-structural mesh alternatively; triangular mesh method is also used to avoid the flow model cusp problem to increase the accuracy of simulation. The working fluid is air; the simulated operating condition is one atmospheric pressure and 300 K. The grid testing results of this study show that the number of grid for the three dimensional numerical analysis of the delta wing is about 1.9×10^5 and the convergence criteria is 10^{-4}. The simulation adopts the finite volume method and uses mass conservation equation, momentum equation, and energy equation, which are matched with no-slip boundary condition. On concerning the thermal effect of the slanted surface around the central hole of a miniature delta wing on the leading-edge vortices, the heat flux at the four slanted surfaces around the square central hole of the delta wing is fixed at Q=10W/m^2 and 100W/m^2 respectively to conduct the grid calculation of the heat flux field of the delta wing [10]. Related boundary condition and initial condition provided by the experimental flow condition would be set in numerical study and confirmed by experiments finally.

The basic fluid governing equations applied at an incompressible flow condition are as follows:

Mass conservation equation:

$$\nabla\cdot\left(\rho\vec{V}\right)=\mathbf{0} \tag{1}$$

Momentum equation:

$$\rho\frac{D\vec{V}}{Dt}=-\nabla P+\rho\vec{g}+\mu\nabla^2\vec{V} \tag{2}$$

Here, ρ is density ; $\vec{V}$ is velocity vector ; μ is fluid viscosity ; P is pressure.

Energy conservation equation:

$$\nabla \bullet (\rho \vec{V} h_0) = \nabla \bullet (K_{eff} \nabla T) + \left[\frac{\partial (u\tau_{xx})}{\partial x} + \frac{\partial (u\tau_{yx})}{\partial y} + \frac{\partial (u\tau_{zx})}{\partial z} \right] + \left[\frac{\partial (v\tau_{xy})}{\partial x} + \frac{\partial (v\tau_{yy})}{\partial y} + \frac{\partial (v\tau_{zy})}{\partial z} \right] + \left[\frac{\partial (w\tau_{xz})}{\partial x} + \frac{\partial (w\tau_{yz})}{\partial y} + \frac{\partial (w\tau_{zz})}{\partial z} \right] + S_k \quad (3)$$

h_o is total enthalpy ; K_{eff} is the effective thermal conductivity of the material ; ι_{ij} is the viscous stress tensor ; S_k is the external sources.

3 Results and Discussion

For realizing the impact of temperature and pressure to the fluid properties at various altitudes such as changes in the fluid viscosity, density, and gas flow velocity etc., this study chooses to use the dimensionless parameter Reynolds number, Re, as the control conditions of the flow field and the simulation analyses are carried out at the control conditions of the flow field of Reynolds number Re $=2.64\times10^3$ and 8.84×10^3 respectively. Because the research results of the micro-delta wing in this study will be applied to the attitude control of micro-satellite in the future, taking into account of the flow field changes on the wing surfaces, which are caused by factors such as actual radiation/heat control on the wing surfaces, this study will conduct analyses for the effect of the velocity field and the temperature field to the flow field of AOA and AOS for the two cases of heating the slanted surfaces of the central hole with Q=100W/m^2 and 10W/m^2.Here, the angle of attack (AOA) is used to describe the angle between the chord line of the wing of a fixed-wing aircraft and the vector representing the relative motion between the aircraft and the atmosphere in aerodynamics [11]. In addition, the angle of sideslip (AOS) relates to the rotation of the aircraft centreline from the relative wind [12]. First, at flow field, Re=2.64×10^3, Fig. 3(a), AOA 10°and AOS 0°, and Fig. 3(b), AOA 25° and AOS 0°, are the velocity and temperature distribution diagrams for the slanted surfaces of the central hole at heating of Q=100W/m^2. Fig. 3(a) shows the temperature distribution of the slanted surfaces of the central hole. Because there exists a larger velocity current at the central region of the lower slant surface and the convection thermal

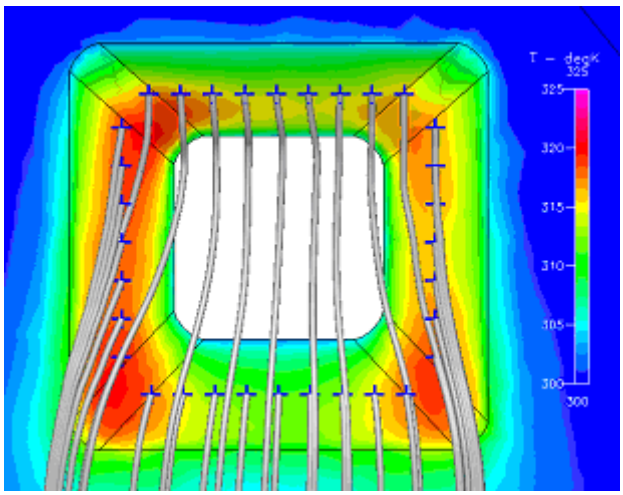

(a)AOA 10° and AOS 0°

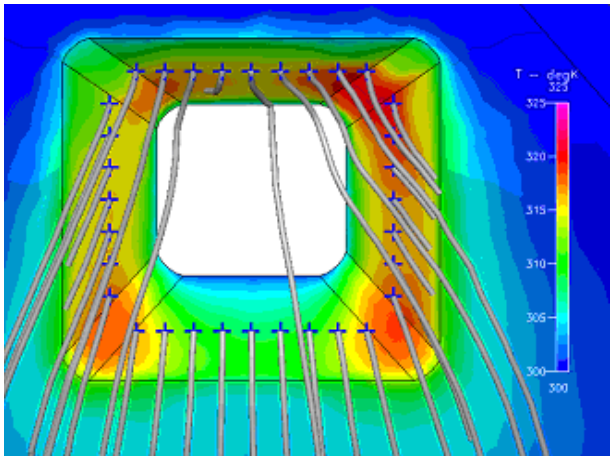

(b) AOA 25° and AOS 0°

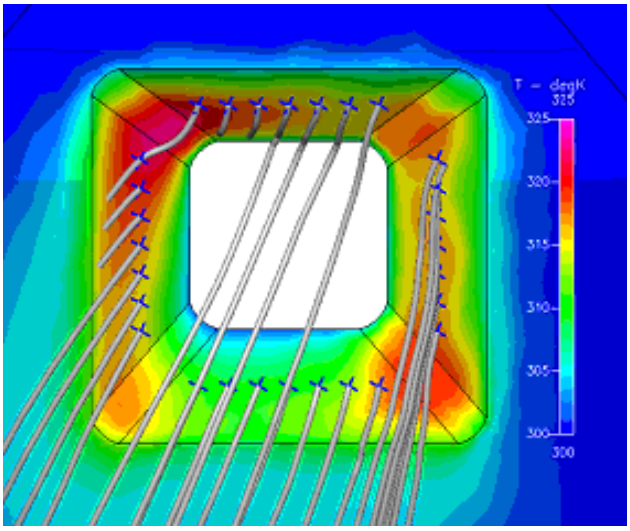

(c) AOA 25° and AOS 25°

Fig.3 The velocity and temperature distribution diagram of the slanted surface of the central hole at Re=2.64×103 and Q=100W/m^2

effect will be enhanced accordingly, the temperature distribution will be lower[6].

However, because a larger temperature gradient exists at the corner of the central hole, the velocity gradient at that point should be larger as well.

Fig. 3(b) shows that there exists uneven temperature distribution on the slanted surfaces of the central hole. This is because an unstable flow field appears around the area; however, the velocity and temperature gradient is still larger at the lower corner of the central hole.

Similarly, when the delta wing is at an AOA of 25° and an AOS of 25°, there exists uneven temperature distribution on the slanted surfaces of the central hole due to unstable flow field as shown in the results of Fig. 3(c).

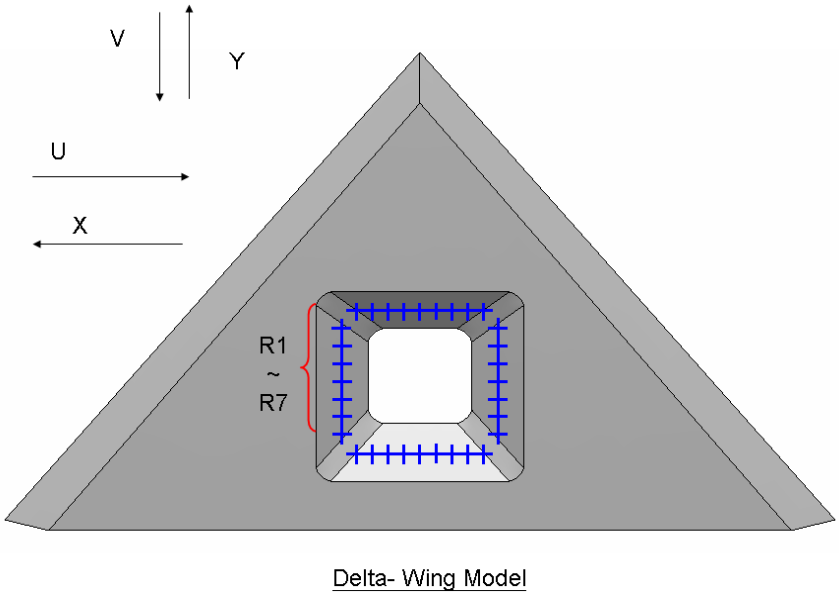

Fig.4 The equal spacing R1-R7 positions on the left slanted surface of the central hole

In order to further understand the thermal flow field on the slanted surfaces of the central hole of a miniature delta wing, seven points are selected at the center of the left slanted surface of the central hole; from the top corner of the left slanted surface (R1) to the bottom corner (R7) with equal spacing, which are marked as R1-R7, as shown in Fig. 4. The U and V direction velocity changes along the normal line direction of the slanted surface are analyzed for these positions.

Fig. 5 shows the results of the U and V velocity distribution of the flow field on the slanted surfaces of the square central hole at different distances from the slanted surface when Re = 2.64 × 10^3, AOA of 5°, AOS of 0°, and the heat transfer of Q = 100W/m^2.

The results of Fig. 5(a) show that there exists a huge velocity differences within a distance of 2cm from the slanted surface, which indicates the existence of a larger unstable flow field due to the development of the vortex structure.

Additionally, because the U direction velocity of R7 at the position of 2cm from the slanted surface is roughly zero, the R7 position must be the vortex radius of the wing tip vortex structure at R7. The U velocity approaches zero at a distance of 8 cm from the slanted surface of the central hole, which indicates that the external flow field is not affected by the interaction between the flow field at the central hole of the wing surface and the wing tip vortex structure.

On the other hand, judging from the V velocity distribution of Fig. 5(b), a larger velocity gradient exists within 2cm from the slanted surface. This study investigates and analyzes the impact of AOA and AOS to the temperature effect under the condition of flow field, Re = 2.64×10^3 and Q=10W/m^2 and 100W/m^2 on the four slanted surfaces of the central hole. It can be seen from the

results of Fig. 6: the temperature of the four slanted surfaces shows a level distribution at a flow field of $Re=2.64\times10^3$ and heat flux of $Q=10W/m^2$, which indicates that there is no significant change of temperature, when AOA changes. When the heat flux is raised to $Q=100W/m^2$, the impact of AOA to temperature is exhibited markedly, among which the changing relationship between temperature and AOA is most pronounced on the slanted surface underneath the central hole.

Similarly, the impact of AOS to the temperature of the four slanted surfaces are investigated and analyzed under the condition of subjecting the central slanted surface to a heat flux of $Q=10W/m^2$ and $100W/m^2$.

The results of Fig. 7 show: when the flow field is $Re=2.64\times10^3$ and the heat flux is $Q=10W/m^2$, the impact of AOS to the temperature effect is not significant; while the heat flux reaches $Q=100W/m^2$, there exhibits a significant change, which indicates that there is significant impact in the changes of temperature from AOA and AOS of the delta wing at high heat flux.

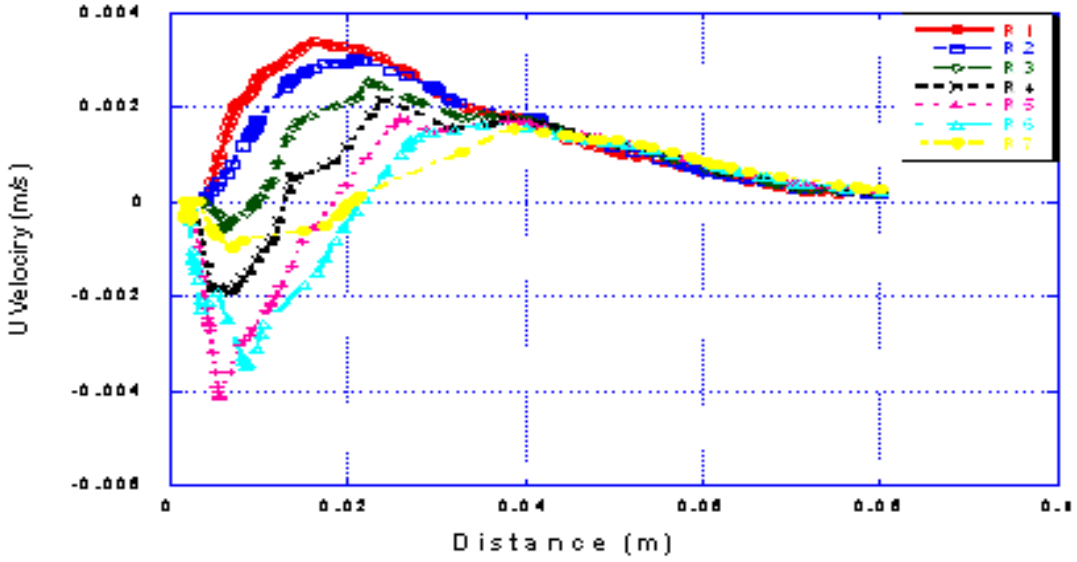

(a)U direction velocity

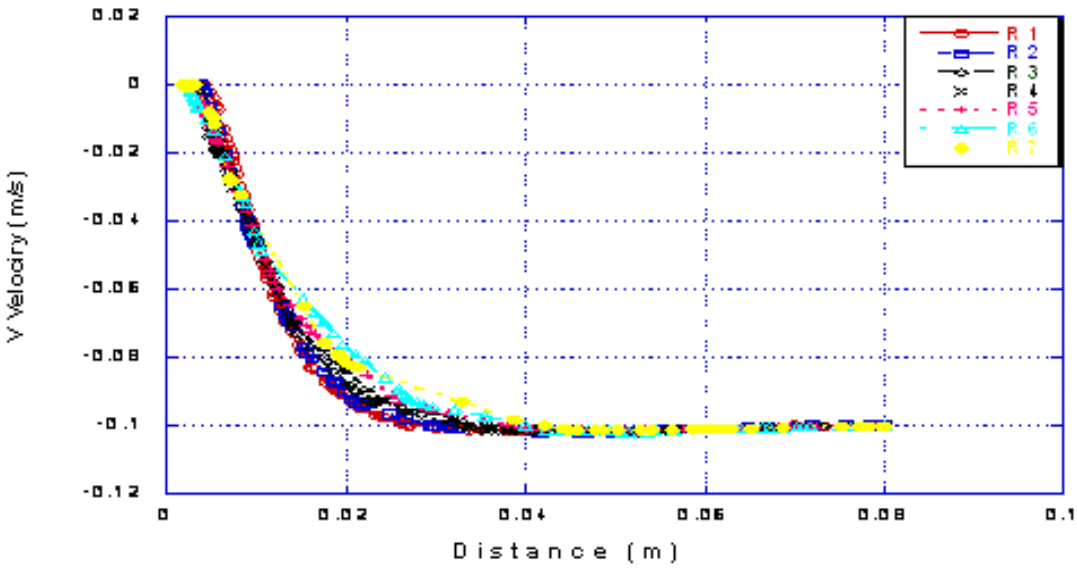

(b) V direction velocity

Fig.5 The velocity distribution at different locations on the slanted surfaces of the central hole under the condition of Re=2.64×10^3, AOA 5° and AOS 0°, and Q=100W/m^2

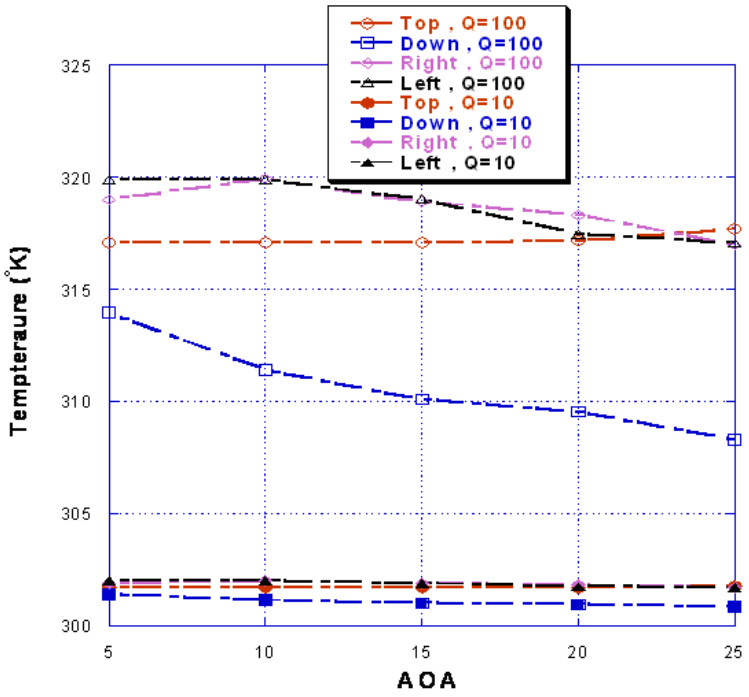

Fig.6 The diagram of the relationship between AOA and temperature on the four slanted surfaces of the central hole of the delta wing under the conditions of flow field Re=2.64×10^3, and Q=10W/m^2 and Q=100W/^{2}

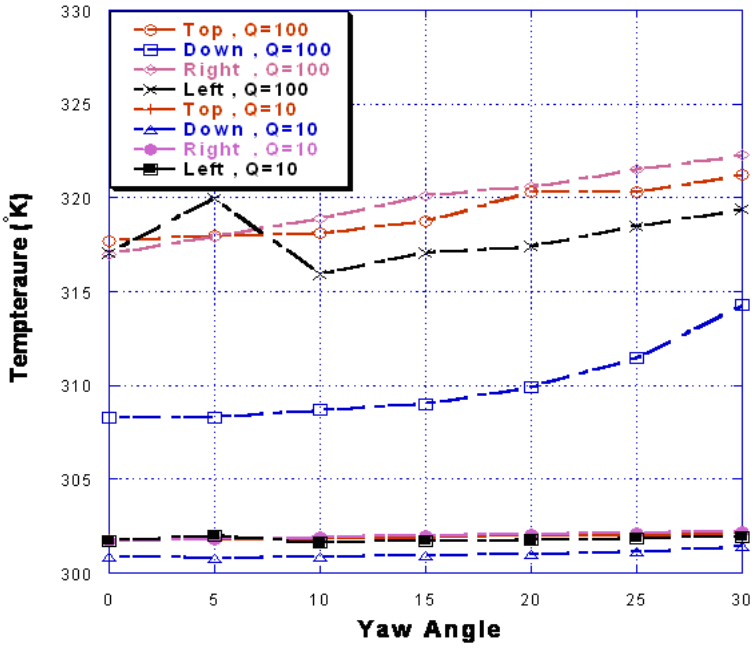

Fig.7 The diagram of the relationship between AOS and the temperature distribution on the four slanted surfaces of the central hole of the delta wing under the conditions of flow field Re=2.64×10^3, and Q=10W /m^{2}and Q=100W/m^2

This study also investigates the impact of AOA and AOS to the temperature effect under the conditions of raising Reynolds number to Re=8.84×10^3 and Q=10W/m^2 and 100W/m^2. Fig. 8 shows that there are no significant changes in AOA

effect when the Reynolds number is raised at $Q=10W/m^2$.

While at the heat flux $Q=100W/m^2$, the temperature on the top slanted surface of the central hole rises with the increase of AOA, which is obviously different from the effect of AOA to temperature at Reynolds number $Re=2.64\times10^3$. It shows that the structure of the flow field has changed significantly at this time.

Also, at $Q=100W/m^2$, when AOA increases to 10°, the increase of AOA will cause the rise of temperature accordingly, which shows that the structure of the vortex flow field on the delta wing is rather weak and the generation of the flow velocity is also lower.

When AOA is larger than 10°, the impact on the wall surface temperature of the central hole caused by the increase of AOA is different. The top wall surface temperature of the central hole rises with the increase of the AOA, which is different from the temperature changing trend of the other three surfaces. It shows that the vortex structure has produced asymmetric flow field under the interaction of the flow field of the central hole of the delta wing; and the near field velocity on the top wall surface of the central hole should be lower than the other three surfaces.

As a result, the thermal convection effect on the top wall surface should be weaker than the other three surfaces. Furthermore, the effect of AOS on the temperature distribution of the four slanted surfaces are investigated and analyzed under the condition of subjecting the central slanted surfaces to a heat flux of $Q=10W/m^2$ and $100W/m^2$, at $Re=8.84\times10^3$.

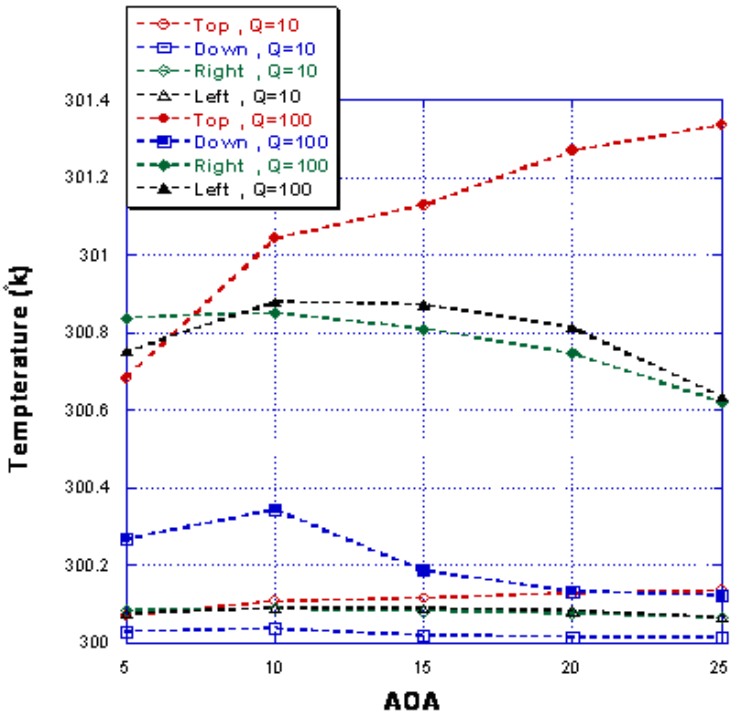

Fig.8 The diagram of the relationship between AOA and temperature on the four slanted surfaces of the central hole of the delta wing under the conditions of flow field $Re=8.84\times10^3$, and $Q=10W/m^2$ and $Q=100W/m^2$

Fig. 9 shows under the condition of $Q=10W/m^2$, when the flow field velocity is raised to $Re=8.84\times10^3$, the changes of AOS seems to have no significant impact on the temperature distribution. While raising the heat flux to which the wall surface is subjected to $Q=100W/m^2$, there are significant impact on the temperature changes under the influence of large AOS.

According to the boundary layer theory, the separation state of the boundary layers at the leading edge of the delta wing will change. The leading edge vortices on both sides of the lee side of the delta wing will be distributed symmetrically without disturbances. Therefore, whether it is before or after the separation of the flow field, if disturbances to separate flows are generated using an actuator or a sensor [13] which matches the thickness of the boundary layer, to influence the flow around the delta wing, the symmetry of the vortex can be broken to produce a torque to control the flight

manoeuvre such as rolling, yawing, and pitching etc. [13].

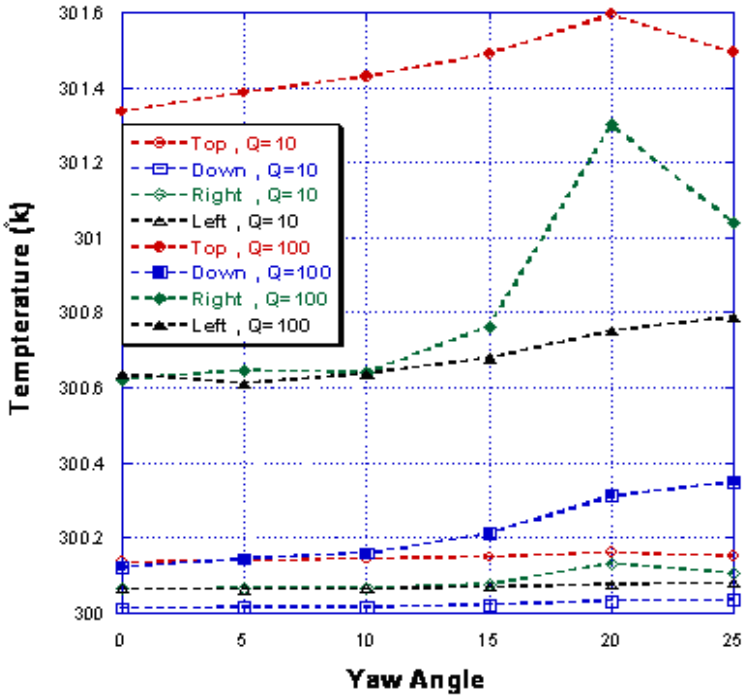

Fig.9 The diagram of the relationship between AOS and the temperature distribution on the four slanted surfaces of the central hole of the Delta wing under the conditions of flow field Re=8.84×10^3, and Q=10W/m^2 and Q=100W/m^2

Fig. 10 (top figure) shows the flow field intensity diagram of the vortex structure at the centre cross section position of the central hole. It shows that the structure of the vortex is intact at this point of time in the figure. However, when the vortex develops towards downstream, the changes of the thermal boundary layers which are caused by the heat transfer will induce interactions between the vortices developed between the wings and the jets from the central hole and further break down the vortex structure and induce asymmetric flow field. Fig. 10 (bottom figure) shows that there exists significant effect on the flow field of the delta wing from the thermal effect under the condition of high angle of attack (HAOA) [14] and high Reynolds number flow field. In general, stable leading edge vortices on a delta wing can improve the aerodynamic performance effectively; while vortex breakdown can lead to a sharp fall in the lift.

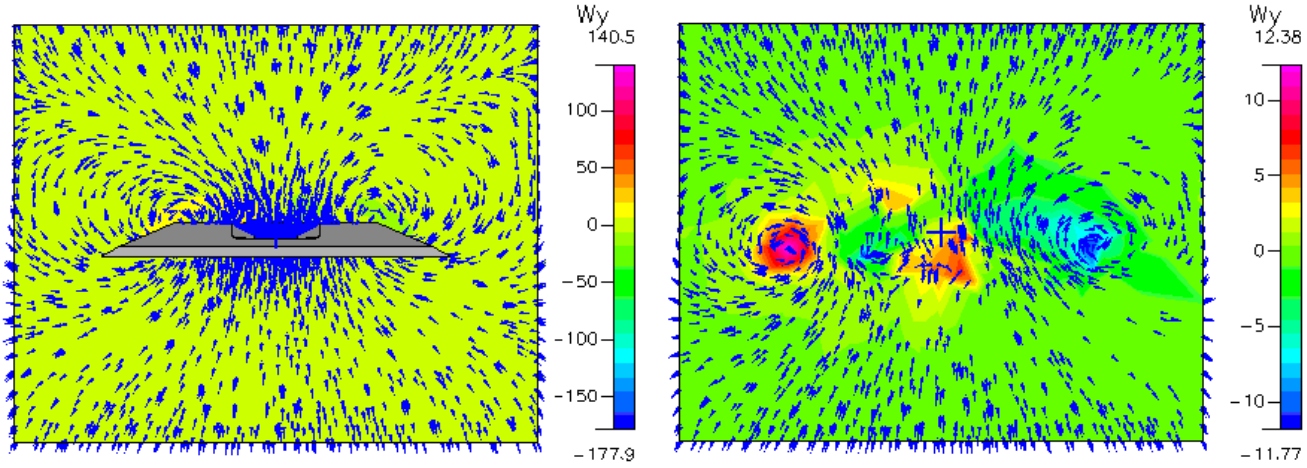

Fig.10 (top figure) the vortex flow field at the center position of the central hole (bottom figure) the vortex flow field at the tip of the delta wing

At HAOA, vortex contributes at least 40% of the total lift [15]. If shear stress sensors are placed within the boundary layers, the instantaneous fluid separation line can be detected and micro-actuators can be activated to control the air flow in the separation region within the boundary layers, thereby changing the vortex structure to produce the necessary torque for pitching / rolling / swaying, which is needed to control the aircraft without the need of the traditional wing control and the required hydraulic or electrical control system: these micro-actuators only need to move 1 to 2 mm to obtain the desired results[15].

To summarize the above discussions, because there is significant velocity and pressure gradient around the corner on the bottom slanted surface of the central hole in the delta wing, it is the region of which the development of vortex flow field is most pronounced and is the recommended thermal control location of the future. These findings will be useful to optimize slot at leading edge [16] and improve the knowledge of the link between mass flow rate and velocity jet exited for defining the new actuator of thermal flow control in the future.

4 Conclusion

This study conducts simulation analyses for the impact of the surface thermal effect on a miniature delta wing to the development of the wing tip vortices to find out the most pronounced region for the changes of the flow field on the wing surfaces. The research results are summarized and described respectively as follows:

The temperature effect under high heat transfer produces significant impact on AOA and AOS of the miniature delta wing aircraft and can cause the occurrence of asymmetric flow field of vortices at the downstream tip of the delta wing. Because a significant velocity gradient and pressure gradient exists around the corner on the bottom slanted surface of the central hole on the delta wing, it is the region of which the development of vortex flow field is most pronounced. These findings could provide information on realizing the thermal effect on the leading-edge vortices over the miniature delta wing for future optimal flow control.

Acknowledgements

This study was supported by the National Science Council of the Republic of China, Taiwan, for financially supporting this research under Contract No. NSC 99-2221-E-197-017.

References:

[1] Lee YK, Kim HD, Vortical flows over a delta wing at high angle of attack, *Journal of Mechanical Science and Technology*. Vol.18, No.6, 2004, pp.1042-1051.

[2] Gresham NT, Wang Z, Gursul I, Vortex dynamics of free-to-roll slender and nonslender delta wings, *Journal of Aircraft*, Vol.47, No.1, 2010, pp.292-302.

[3] Elkhoury M, Nakad Z, Surface streamlines and normal-to-plane motion adjacent to a delta-wing planform, *Journal of Aircraft*, Vol.46, No.4, 2009, pp.1440-1443.

[4] Zhang W, Ye Z, Effects of leading-edge vortex on flutter characteristics of high sweep angle wing, *Hangkong Xuebao/Acta Aeronautica et Astronautica Sinica*, Vol.30, No.12, 2009, pp. 2263-2268.

[5] Eibeck PA, Eaton JK, Heat transfer effects of a longitudinal vortex embedded in a turbulent boundary layer, *Journal of Heat Transfer*. Vol.109, No.1, 1987, pp.16-24.

[6] Pauley WR, Eaton JK, The effect of embedded longitudinal vortex arrays on turbulent boundary layer heat transfer, *J. of Heat Transfer,* Vol.116, No.4, 1994, pp.871-878.

[7] Fiebig M, Kallweit P, Tiggelbeck S, Heat transfer enhancement and drag by longitudinal vortex generators in a channel flow, *Experimental Thermal and Fluid Science,* Vol.4, 1991, pp.103-114.

[8] Ye X, Yang Y, Flutter of delta wing under aerodynamic heating, *Journal of Southwest Jiaotong University,* Vol.43, No.1, 2008, pp.62-66.

[9] Michael W, Robin S, Computational fluid dynamics analysis of microbubble formation in microfluidic flow-flcusing devices, *Microfluidics and Nanfluidics,* Vol.3, No.2, 2007, pp.195-206.

[10] Wang CT, Sun JM, Leu GH, Miao JJ, Analysis of central-hole effect on wing-tip vortex flow for miniature delta wing, *Journal of C.C.I.T.* Vol.37, No.1, 2008, pp. 197-202.

[11] Gracey William, *Summary of methods of measuring angle of attack on aircraft, NACA Technical Note (NASA Technical Reports)*. 1958, pp. 1-30.

[12] Hurt H, H Jr, Aerodynamics for Naval Aviators. U.S. government printing office, Washington D. C.: U.S. Navy, Aviation Training Division. 1960, pp. 284-285.

[13] Lee GB, Shih C, Tai YC, Tom T, Ho CM, Robust vortex control of a delta wing using distributed MEMS actuators, *AIAA Journal of Aircraft*. Vol.37, No.4, 2000, pp.697-706.

[14] Simon JM, Blake WB, Missile datcom: high angle of attack capabilities, *AIAA-99-4258*. 1999, pp.1-11.

[15] Lee GB, Shih C, Ho CM, The control of a delta wing by micromachined sensors and actuators, 13th U. S. *Congress of Applied Mechanics*, Gainesville, USA, June 21-26, 1998.

[16] Jiang F, Lee GB, Tai YC, Ho CM, A flexible micromachine-based shear-stress sensor array and its application to separation-point detection, *Sensors et Actuators*. Vol.79, 2000, pp. 194-203.